11,12

Tetragonal nanocrystalline phases in oxides Re_2O_3

© I.M. Smytko, V.V. Kedrov

Osipyan Institute of Solid State Physics RAS,
Chernogolovka, Russia

E-mail: shim@issp.ac.ru

X-ray diffractometric studies of the structural state of simple rare-earth oxides Gd_2O_3, Sm_2O_3 and Eu_2O_3 were carried out, synthesized by different methods, at the first stages of crystal formation. It was found that the first crystalline phase of these compounds in the nanocrystalline state is not a known cubic modification with the spatial symmetry group S.G. Ia-3 (206), but tetragonal phases, whose spatial groups are not established due to the small number of strong reflexes in the nanostate. It is also shown that the same tetragonal phases are formed in industrial powders of these compounds subjected to long-term storage.

Keywords: synthesis of Re_2O_3, glycine-nitrate method, nanocrystalline state, X-ray diffraction research methods, phase transitions.

1. Introduction

Much attention is being paid at present to studying the structural study and phase transformations of nanoscopic systems with change of crystallite size. Simple and complex oxides, as well as fluorides of rare earth elements (REE) are interesting from this viewpoint. The interest in REE oxides and fluorides is primarily due to the fact that many of them have scintillation and phosphor characteristics [1–13].

We have previously performed detailed structural studies of a number of rare-earth oxide compounds synthesized from the amorphous precursor state [14–28]. We have demonstrated that their structure greatly depends on crystallite size. Thus, the $LuBO_3$, $Eu_2(MoO_4)_3$, $ScBO_3$ and $TbBO_3$ compounds [14–16], obtained from amorphous precursors, are characterized by cyclic structure rearrangement with increase of crystallite size. In these compounds, not the phase which is the equilibrium one for the given temperature, but the high-temperature phase is the first to crystallize upon precursor heating. In the course of subsequent annealing accompanied with crystallite growth, this phase first transforms into an equilibrium low-temperature phase, known for the microcrystalline state, while with further increase of annealing temperature it again transforms into the high-temperature one, but this time an equilibrium one. The main reason for such cyclic structural rearrangements in the synthesis of complex REE oxides is assumed to be an increase in the chemical potential due to the increased energy of atoms on the surface of crystallites, the proportion of which increases with decreasing size.

The role of surface atoms is also clearly manifested in the compaction of nanopowders of simple REE oxides by the appearance of additional phases at certain sizes of nanocrystallites, which disappear with the subsequent growth of crystallites with an increase in the annealing temperature of [28].

The above structural effects of simple and complex REE oxides were obtained on samples synthesized by simple exchange interaction of nitrates $Re(NO_3)_3$ with boric acid H_3BO_3 in the aquatic environment. There are many methods of synthesis of REE oxides [29–37]. This is sol−gel [29], polyol [30], flame spray pyrolysis [31,32], laser ablation [33], hydrothermal [34,35] and direct deposition [36]. An interesting result was obtained by us [37] for gadolinium oxide samples without doping (Gd_2O_3) and doped with europium atoms ($Gd_2O_3 : 2\%Eu^{3+}$) obtained in the combustion mode by the glycine-nitrate method [38,39]. For this purpose, in the case of the synthesis of Gd_2O_3, glycine was added to an aqueous solution of gadolinium nitrate salts in the amount necessary to carry out the process of

$$Gd(NO_3)_3 + 1.55C_2H_5NO_2 \text{ (glycine)}$$
$$\rightarrow 0.5Gd_2O_3 + 3.11CO_2 + 3.88H_2O + 2.28N_2$$
$$+ 3.11CO_2 + 3.88H_2O + 2.28N_2,$$
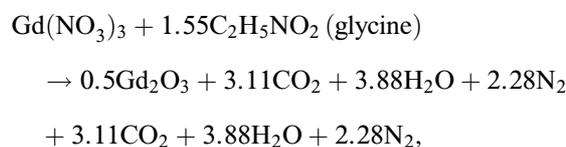
and in the case of synthesis $Gd_2O_3 : Eu^{3+}$ glycine was added to aqueous solutions of gadolinium and europium nitrate salts, taken in a molar ratio of 98 : 2, in the amount necessary to carry out the process of

$$0.98Gd(NO_3)_3 + 0.02Eu(NO_3)_3 + 1.55C_2H_5NO_2 \text{ (glycine)}$$
$$\rightarrow 0.5(Gd_{0.98}Eu_{0.02})_2O_3 + 3.11CO_2 + 3.88H_2O + 2.28N_2.$$
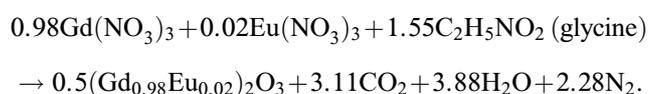
Glycine was taken with a 20% excess of the stoichiometric amount. After evaporation of the water, combustion reaction was initiated by heating the mixture. At the

end of the combustion process, the resulting highly dispersed nanocrystalline product contained carbon impurities, for the removal of which the product was annealed in air at $700°C$ during 0.5 h. As a result, a series of samples differing in temperature and synthesis time was obtained. The most interesting result was obtained at a furnace temperature equal to $650°C$ and a synthesis time equal to 20 min. The essence of this result is shown in Figs. 1 and 2 and consists in establishing the presence of a new nanoscopic tetragonal phase preceding the formation of the cubic modification Re_2O_3 known for all oxides.

Fig. 1 shows the spectra of the sample $Gd_2O_3 : 2\%$ Eu^{3+} synthesized at $T = 650°C$ during 20 min. The spectrum *1* refers to the state formed immediately after synthesis. Such a spectrum corresponds to the nanostate of a known cubic phase with the spatial symmetry group S.G. Ia-3. The spectrum *2* describes the state of the sample after a year of exposure at room temperature in the air. Such a spectrum corresponds to a tetragonal phase with lattice parameters $a = b = 11.900$ Å, $c = 11.307$ Å, $V = 1601$ Å^3. The tetragonal phase is thermodynamically equilibrium, which is confirmed by the transition of the sample back to the initial nanoscopic cubic phase when the annealing temperature increases to $400°C$.

In the case of obtaining Gd_2O_3 without doping with europium under the same synthesis conditions, a two-phase state is obtained from tetragonal and cubic nanoscopic phases, see spectrum *2*, Fig. 2. Annealing of such a sample at a temperature of $650°C$ is accompanied by the disappearance of the tetragonal phase while maintaining the cubic one.

A natural question arises: „The formation of the tetragonal phase at the initial stages of the synthesis of Gd_2O_3 is due to the glycine-nitrate method in the combustion mode or is this the general state of REE oxides at the first stages
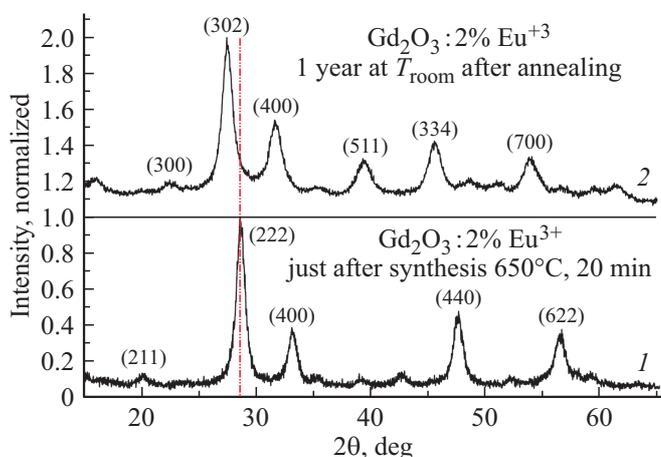
Figure 2. Diffraction spectra of samples Gd_2O_3 and $Gd_2O_3 : 2\%$ Eu^{3+} obtained at the synthesis temperature, equal to $650°C$, and synthesis time equal to 20 min: *1* — $Gd_2O_3 : 2\%$ Eu^{3+} after prolonged exposure of the sample at room temperature; *2* — the spectrum of the sample Gd_2O_3 obtained immediately after synthesis. *3* — spectrum of the sample represented by the spectrum *2*, after annealing at a temperature of $650°C$ for 1st hour.

of the formation of crystalline phases, regardless of the synthesis method?“ This study is devoted to the answer to this question.

2. Samples and experimental procedure

4 types of nanoscopic samples were studied.

The first type — are samples of samarium oxide Sm_2O_3. They were obtained in the combustion mode by the glycine-nitrate method [38,39]. To do this, glycine was added to an aqueous solution of nitrate salts of samarium in the amount necessary to carry out the process of

$$Sm(NO_3)_3 + 1.55C_2H_5NO_2(glycine)$$
$$\rightarrow 0.5Sm_2O_3 + 3.11CO_2 + 3.88H_2O + 2.28N_2$$
$$+ 3.11CO_2 + 3.88H_2O + 2.28N_2.$$
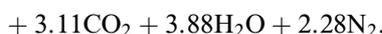
The amount of glycine was taken with a 20% excess of the stoichiometric amount. After water evaporation, the combustion reaction of the resulting product was initiated by placing the precursor in an furnace with a given synthesis temperature. The synthesis temperature was $\sim 300°C$, the synthesis time was 20 min.

The second type of samples — are ready-made industrial powders of samarium oxide Sm_2O_3 and gadolinium oxide Gd_2O_3. Gadolinium oxide powder had an ultra high purity (UHP) and was manufactured at the factory „Giredmet“ in 2000 according to technical conditions No. 48-4-524-90. Samarium oxide powder was also manufactured at the „Giredmet“ factory in 2006.

Figure 1. Diffraction spectra of the structural state of the synthesized sample $Gd_2O_3 : 2\%Eu^{3+}$, obtained at a synthesis temperature of $650°C$ and a synthesis time of 20 min: *1* — immediately after synthesis; *2* — a year later.

The third type — are samples of Eu_2O_3 obtained in the nanostate by the sol–gel method. For this purpose, the original UHP-powder Eu_2O_3 was mixed with saltpeter (NH_4NO_3) and heated to the temperature of formation of a transparent solution-melt. Further, the melt solution was rapidly heated to $700-1100°C$, which led to the formation of a significant amount of gaseous products and a solid product —precursor. Then the precursor was annealed in an furnace at a temperature $300-500°C$ for several tens of minutes. As a result, a nanoproduct was obtained, which was studied by X-ray diffraction methods.

The fourth type — are samples of Eu_2O_3 obtained in the nanostate in the combustion mode of the $Eu(NO_3)_3 + CH_2OH - CH_2OH$ (ethylene glycol). To carry out this synthesis in an aqueous solution of europium nitrate containing $10\,mmol$ salts, $1.10\,g$ ($17.7\,mmol$) of ethylene glycol was added, and the resulting solution was carefully heated until the water evaporated completely. The continued heating of the solid precipitate led to its ignition and the formation of a nanopowder Eu_2O_3, containing an admixture of carbon.

The structural state of the samples was recorded on an X-ray diffractometer D500 (Siemens) using the Bragg–Brentano scheme. Monochromatized $CuK\alpha$ output graphite monochromator radiation was used. Temperature changes were carried out in a laboratory furnace SNOL-6.7/1300 and were characterized by successive isothermal annealing in air for 0.2 to 2 h at each temperature point, depending on the change in structure in the previous annealing. At the same time, the temperature interval between successive annealing was $25-100°C$.

3. Experimental results and discussion

Fig. 3 shows the spectra of the sample Sm_2O_3 synthesized in the combustion mode by the glycine-nitrate method. The spectrum *1* refers to a sample first annealed at a temperature of $200°C$, and then at $300°C$ for 2 h. During these annealing, the spectra coincided with the spectrum of the initial state immediately after synthesis. The spectrum *2* refers to the same sample additionally annealed at a temperature of $350°C$ for the same 2 h. There is a noticeable movement of the peak of the strongest reflex towards the lower corners. The spectrum *3* displays the state of the sample annealed at a temperature of $400°C$. The position of the peaks of all strong reflexes in this case corresponds to the known cubic modification Sm_2O_3, which is confirmed by the spectrum *4*, which displays the state of the sample after successive annealing every $50°C$ before the start formation of a monoclinic modification, at a temperature $750°C$.

Further annealing of the sample leads to a gradual transition of the cubic modification into the known monoclinic phase, see Fig. 4. The figure shows the half-widths of the reflex (222) for three annealing temperatures of 750, 850 and $950°C$. Since the half-width of the reflex in the
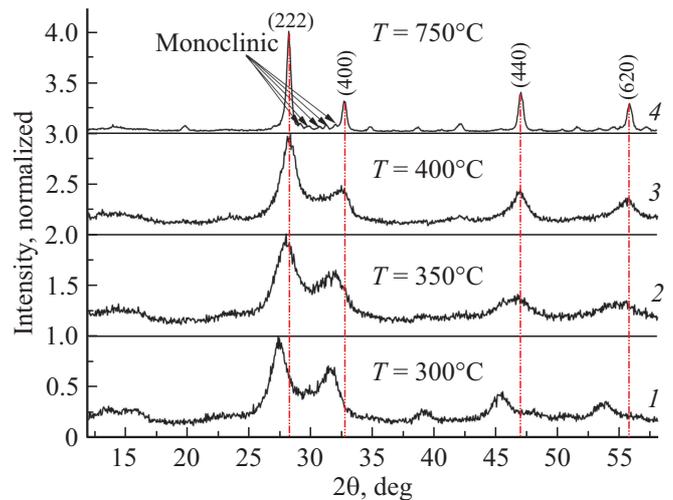
Figure 3. Temperature changes in the diffraction spectra of the sample Sm_2O_3 synthesized by the glycine-nitrate method.
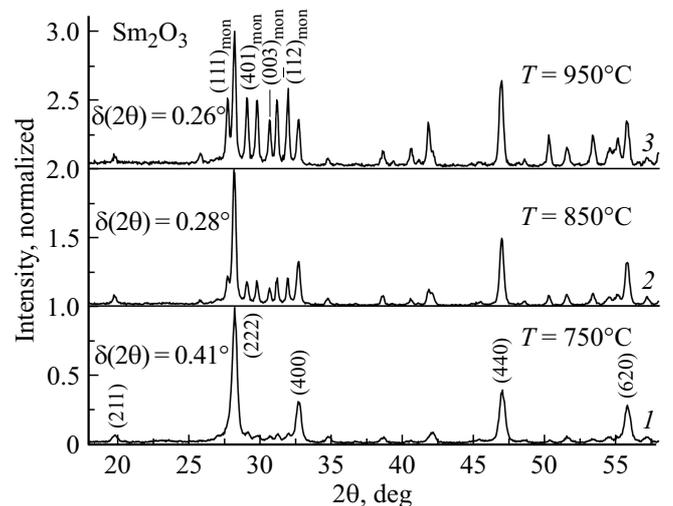
Figure 4. The sequence of changes in the diffraction spectra during the transformation of the sample Sm_2O_3 from cubic to monoclinic modification.

nanostate reflects the average size of the crystallites, a decrease in the half-width of the reflexes with an increase in the annealing temperature means an increase in their average size. The figure shows that while the proportion of the monoclinic phase increases, the half-width of the reflex (222) decreases, while the center of gravity of the reflex remains. The latter means that the first transformations into the monoclinic phase at lower temperatures are experienced by crystallites of minimal diameter. As the annealing temperature increases, larger crystallites also enter the monoclinic phase. This behavior of the transition „cubic phase → monoclinic phase" corresponds to a phase transition of the first kind. Thus, from Figs. 3 and 4, we can conclude that both for Gd_2O_3, and for Sm_2O_3 the formation of a cubic modification in the nanocrystalline state
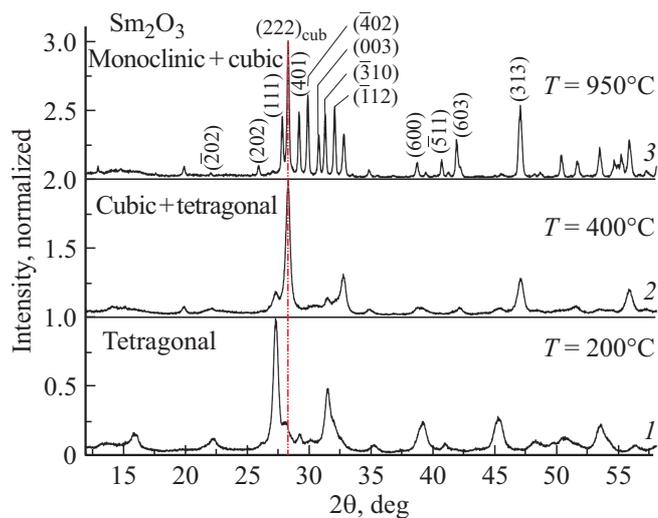
Figure 5. Diffraction spectra of Sm_2O_3 „powder from a jar" for different annealing temperatures of the same sample. The spectrum *1* — is the spectrum of the initial state of the powder. The spectrum *2* displays the structural state of the powder after successive annealing every $50°C$ for 2 h at each temperature point. The spectrum *3* displays a partial transition to a monoclinic modification of the cubic phase.
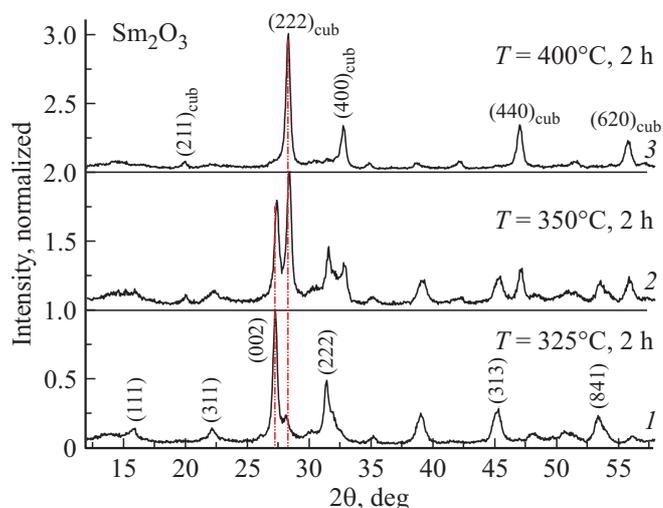
Figure 6. Diffraction spectra of Sm_2O_3 „powder from a jar" near the phase transition from the tetragonal phase to the traditional cubic one.

is preceded by the formation of a lower symmetric phase. The latter follows from the larger number of reflexes for this phase and the shift of reflexes to the small-angle part of the spectrum with respect to the reflexes of the cubic phase, displayed on the spectra *1* and *3* in Fig. 3. The symmetry of this phase will be established below in the text.

New unexpected results for Sm_2O_3 were obtained on samples „from the jar". As described in section 2, samarium oxide powder was manufactured at the „Giredmet" factory in 2006. Fig. 5 and 6 show the diffraction spectra of

the initial state of the powder and their transformation during subsequent annealing. Attention is drawn to the discrepancy between the initial spectrum and the spectrum of the cubic phase formed during powder annealing at $T = 400°C$. The symmetry of the cell parameters was found using the Treor90 program. The following parameters were determined: tetragonal symmetry, $a = b = 15.9767$ Å, $c = 6.5716$ Å, $V = 1677.4$ Å^3. Indices of reflexes of this phase are shown in Fig. 6, spectrum *1*. The obtained result unambiguously shows the existence of a new previously unknown tetragonal phase for both Gd_2O_3 and Sm_2O_3.

The detection of the tetragonal phase immediately during the industrial synthesis of Sm_2O_3 posed us a question: „And in industrial synthesis of other rare earth oxides, is the formation of such phases also possible?" To confirm this assumption, the diffraction spectrum for Gd_2O_3 „was removed from a jar" prepared using the same technology as Sm_2O_3 in 2000. The result is shown in Fig. 7. Intense reflexes of black — are reflections of the powder „from the jar". The gray spectrum — is the spectrum of the tetragonal phase obtained by the glycine-nitrate method and shown in the spectrum *2* Fig. 1. There is a two-phase state of tetragonal and cubic phases for industrial powder Gd_2O_3 „from the jar". Thus, it is possible to make an assumption about the existence of a tetragonal phase for many simple REM oxides in the nanostate.

To confirm this assumption, additional experiments were carried out on Eu_2O_3 nanopowders obtained by the glycine-nitrate method and the sol−gel method, see section 2. Results are shown in Figs. 8 and 9.

Fig. 8 shows the diffraction spectra of the Eu_2O_3 nanopowder obtained by the glycine-nitrate method. The dynamics of changes in the half-width and centers of gravity of reflexes with the annealing temperature gives grounds to assert that a nanostate is obtained from two phases whose crystallite size does not exceed several nanometers. An increase in the annealing temperature leads to a gradual transition of the phase with a longer lattice period into a
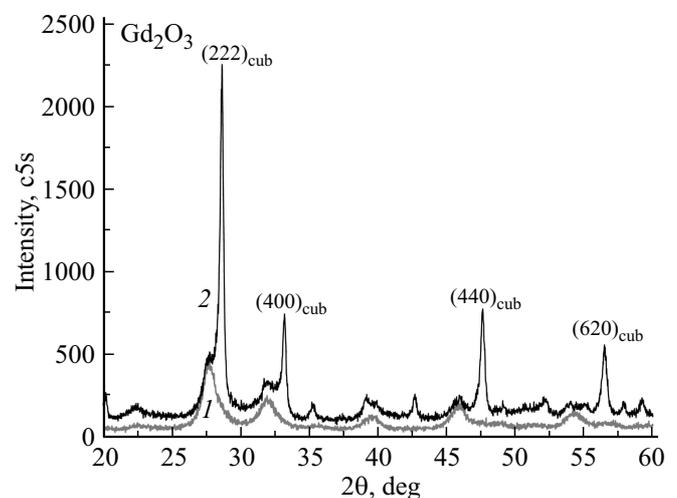
Figure 7. Diffraction spectra Gd_2O_3.
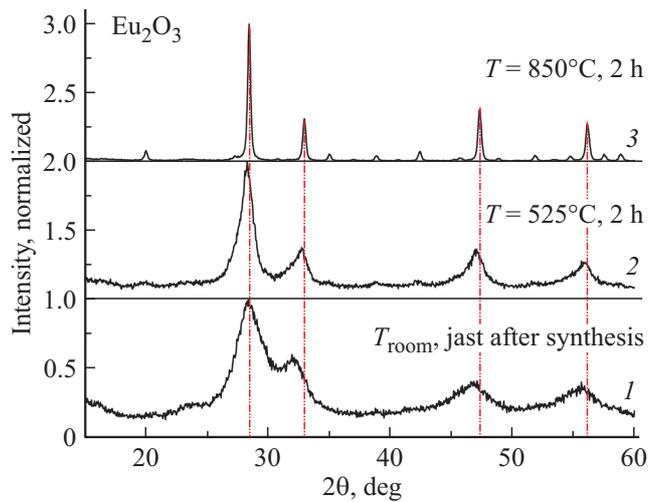
Figure 8. Diffraction spectra of nanopowder Eu_2O_3, obtained by the glycine-nitrate method: *1* — immediately after synthesis; *2* — after successive annealing up to $T = 525°C$; *3* — after successive annealing up to $T = 850°C$.
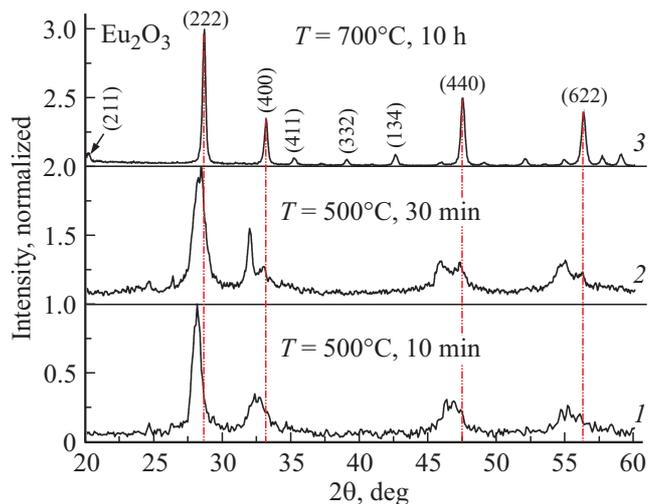
Figure 9. Diffraction spectra of Eu_2O_3 nanopowder obtained by the sol-gel method. (*1*) — after annealing of the initial amorphous precursor at $T = 500°S$ for 10 min; (*2*) — two-phase state after subsequent annealing at $T = 500°C$ for 20 min; (*3*) — after subsequent annealing at $T = 700°C$ for 10 h.

phase that, during high-temperature annealing, corresponds to a known cubic modification with the spatial symmetry group Ia-3 (206) and the lattice parameter $a = 10.859$ Å. Unfortunately, the blurred nature of the reflexes does not allow us to draw any conclusion about the symmetry of the new phase.

Additionally, experiments were carried out on nanopowders Eu_2O_3, obtained by the sol−gel method, see section 2. The experimental results are presented in Fig. 9. It is clearly seen that at the first stages of crystallization, a phase different from the traditional cubic structure is formed. The shift of the reflexes of this phase to the small-angle

diffraction area indicates its larger volume than that of the cubic phase. It is also evident that there are, albeit weak, additional reflexes in the area of $35-45$ deg, which gives us reason to state the difference between this phase and the phase with cubic symmetry. Unfortunately, a very small number of strong reflexes does not allow us to determine the symmetry and lattice parameters of this phase. By analogy with the results of Gd_2O_3 and Sm_2O_3, we can only assume that the symmetry of this phase is also tetragonal.

Summing up the results presented, we draw attention to the fact that the tetragonal phases we found in Gd_2O_3, Sm_2O_3 and Eu_2O_3 does not depend on the synthesis method. They are formed at the first stages of crystallization from the initial precursors and transformed upon heating into a known cubic modification with spatial symmetry S.G. Ia-3. For this reason, they are thermodynamically equilibrium. It can be assumed that not only for the studied Gd_2O_3, Sm_2O_3 and Eu_2O_3 tetragonal phase states are formed in the nanodisperse state, but they can also be formed in other simple oxides of REM.

4. Conclusion

It is experimentally shown that at the first stages of crystallization Gd_2O_3, Sm_2O_3 and Eu_2O_3 tetragonal phases are the first to form from the precusory state in the nanostate. They are thermodynamically equilibrium and, with further high-temperature annealing, they transform into a known cubic modification. It is assumed that the same phases can be formed in other simple oxides of REM.

Conflict of interest

The authors declare that they have no conflict of interest.

References

[1] Z. Wei, L. Sun, C. Liao, J. Yin, X. Jiang, C. Yan, S. Lü. J. Phys. Chem. B **106**, *22*, 10610 (2002).
[2] H. Giesber, J. Ballato, W. Pennington, J. Kolis. J. Inf. Sci. **149**, *1−3*, 61 (2003).
[3] H. Giesber, J. Ballato, G. Chumanov, J. Kolis, M. Dejneka. J. Appl. Phys. **93**, *11*, 8987 (2003).
[4] T. Kim, S. Kang. Mater. Res. Bull. **40**, *11*, 1945 (2005).
[5] J. Lin, Y. Huang, J. Zhang, X. Ding, S. Qi, C. Tang. Mater. Lett. **61**, *7*, 1596 (2007).

[6] L. Chen, Y. Jiang, S. Chen, G. Zhang, C. Wang, G. Li. J. Lumin. **128**, *12*, 2048 (2008).

[7] J. Dexpert-Ghys, R. Mauricot, B. Caillier, P. Guillot, T. Beaudette, G. Jia, P. Tanner, B. Cheng. J. Phys. Chem. C **114**, *14*, 6681 (2010).

[8] J. Li, Y. Wang, B. Liu. J. Lumin. **130**, *7*, 981 (2010).

[9] A. Szczeszak, S. Lis, V. Nagirnyi. J. Rare Earths **29**, *12*, 1142 (2011).

[10] Z. Yang, D. Yan, K. Zhu, Z. Song, X. Yu, D. Zhou, Z. Yin. J. Mater. Lett. **65**, *8*, 1245 (2011).

[11] A. Szczeszak, T. Grzyb, S. Lis, R. Wiglusz. J. Dalton Trans. **41**, *19*, 5824 (2012).

[12] S. Choi, B.-Y. Park, H.-K. Jung. J. Lumin. **131**, *7*, 1460 (2011).

[13] C.R. Ronda, T. Jüstel, H. Nikol. J. Alloys. Compd. **275**−**277**, 669 (1998).

[14] I.M. Shmytko, G.K. Strukova, E.A. Kudrenko. Crystallogr. Rep. **51**, Suppl. *1*, S163 (2006).

[15] I.M. Shmytko. FTT **61**, *2*, 340 (2019).

[16] I.M. Shmytko. FTT **61**, *11*, 2210 (2019).

[17] E.A. Kudrenko, I.M. Shmytko, G.K. Strukova. FTT **50**, *5*, 924 (2008).

[18] I.M. Shmytko, E.A. Kudrenko, G.K. Strukova, N.V. Klassen. FTT **50**, *6*, 1108 (2008) (in Russian).

[19] I.M. Shmytko, E.A. Kudrenko, G.K. Strukova. FTT **51**, *9*, 1834 (2009).

[20] I. Shmytko, G. Strukova, E. Kudrenko. Acta Cryst. A **66**, S230 (2010).

[21] I.M. Shmytko, I.N. Kiryakin, G.K. Strukova. FTT **53**, *2*, 353 (2011).

[22] I. Shmytko. Acta Cryst. A **67**, S533 (2011).

[23] V.V. Kedrov, I.M. Shmyt'ko, S.Z. Shmurak, E.A. Kudrenko, N.V. Klassen. J. Mater. Res. **27**, *16*, 2117 (2012).

[24] I.M. Shmytko, I.N. Kiryakin, G.K. Strukova. FTT **55**, *7*, 1364 (2013); FTT **55**, *7*, 1369 (2013).

[25] E.A. Kudrenko, I.M. Shmytko, G.K. Strukova. FTT **50**, *5*, 924 (2008).

[26] E.A. Kudrenko, I.M. Shmytko, G.K. Strukova. Acta Cryst. A **64**, S427 (2008).

[27] I.M. Shmytko, E.A. Kudrenko, G.K. Strukova, V.V. Kedrov, N.V. Klassen. Z. Kristallogr. **27** (Suppl.), 211 (2008).

[28] I.M. Shmytko, G.R. Ganeeva, A.S. Aronin. FTT **57**, *1*, 129 (2015) (in Russian).

[29] A.G. Murillo, A.M. Ramírez, F.C. Romo, M.G. Hernández, M.D. Crespo. Mater Lett. **04**, *7*, 034 (2009).

[30] A. Müller, O. Heim, M. Panneerselvam, M. Willert-Porada. Res. Bull. **40**, *12*, 2153 (2005).

[31] F. Mangiarini, R. Naccache, A. Speghini, M. Bettinelli, F. Vetrone, J.A. Capobianco. Mater. Res. Bull. **45**, *8*, 927 (2010).

[32] Y. Iwako, Y. Akimoto, M. Omiya, T. Ueda, T. Yokomori. J. Lumin. **130**, *8*, 1470 (2010).

[33] G. Ledoux, D. Aman, C. Dujardin, K. Masenelli-Varlot. Nanotechnology **20**, *44*, 445605 (2009).

[34] G. Liu, G. Hong, J. Wang, X. Dong. J. Alloys Compd. **432**, *1*−*2*, 200 (2007).

[35] Kyung-Hee Lee, Yun-Jeong Bae, Song-Ho Bayeon. Bull. Korean Chem. Soc. **29**, *11*, 2161 (2008).

[36] R. Bazzi, M.A. Flores-Gonzalez, C. Louis, K. Lebbou, C. Dujardin, A. Brenier, W. Zhang, O. Tillement, E. Bernstein, P. Perriat. J. Lumin. **102**, *5*, 445 (2003).

[37] I.M. Shmytko, V.V. Kedrov. FTT **64**, *8*, 1069 (2022) (in Russian).

[38] K.C. Patil, S.T. Aruna, T. Mimani. Solid State Mater. Sci. **6**, *6*, 507 (2002).

[39] K.C. Patil, M.S. Hegde, T. Rattan, S.T. Aruna. Chemistry of Nanocrystalline Oxide Materials: Combustion Synthesis, Properties and Applications. World Scientific, New Jersey (2008). 364 pp.